Available online at www.sciencedirect.com
SCIENCE DIRECT®
Catalysis Today 93–95 (2004) 535–540
CATALYSIS TODAY
www.elsevier.com/locate/cattod

Active sites for heterogeneous catalysis by functionalisation of internal and external surfaces

S.A. French [a,*], A.A. Sokol [a], J. To [a], C.R.A. Catlow [a], N.S. Phala [b], G. Klatt [b], E. van Steen [b]

[a] *Davy Faraday Research Laboratory, The Royal Institution of Great Britain, 21 Albemarle Street, London W1S 4BS, UK*
[b] *Catalysis Research Unit, Department of Chemical Engineering, University of Cape Town, Private Bag, Rondebosch 7708, SA, UK*

Available online 6 August 2004

Abstract

Molecular modelling has the ability to provide the atomistic understanding of processes in catalysis. To be able to investigate the mechanisms of reactions we must first be certain of the active site of the catalyst. In this paper, we outline our recent work on methanol synthesis in which we used the polar surfaces of zincite as a model for the industrial catalyst, before detailing our investigation of Group 11 metals supported on metal oxides. Copper is known to promote industrial catalysis, while silver and gold have also been shown to be active at a much lower weight percent of metal (with gold being the most promising) for both methanol synthesis and the water gas shift reaction. We also present the first systematic study of the stability of Groups 4 and 14 metal impurities in the framework of silicalite. Throughout we assess the effect of the metal dopant on the atomic and electronic structure of the oxide support.

All the work presented here has employed an embedded cluster approach suitable for studying impurities in solid lattices both at internal and external surfaces, which has been implemented in the software ChemShell.

Keywords: Heterogeneous catalysis; Internal and external surfaces; Molecular modelling

1. Introduction

The properties of solids can be altered at both the internal and external surfaces by introducing impurities. This ability to introduce functionalisation impacts on many different areas of chemistry and physics, for example in fuel cell technology and superconducting materials, and it is the ability of transition metals to perform both as redox centres and active sites for catalysis that has had a huge influence on the field of heterogeneous catalysis. The examples given here probe the active sites both on the surfaces and in the pores of metal oxides:

- methanol synthesis on the polar surfaces of zincite,
- supported Group 11 metals on metal oxides,
- functional metal centres in zeolite frameworks.

2. Methodology

As we are interested in localised states in extended systems, such as active sites on internal and external surfaces of heterogeneous catalysts the tools best suited to the problem are embedded molecular cluster approaches. Two particular embedding schemes tuned for the study of dense metal oxides and microporous aluminium silicates were implemented in the computational chemistry environment code ChemShell (see [1–4] and references therein).

Both schemes employ hybrid quantum mechanics/molecular mechanics (QM/MM) methodology whereby we identify:

(i) the proposed active site, and treat it at a high level of theory, i.e. QM;
(ii) the remaining system, which is only subject to minor perturbation by the active site and therefore can be described by simple parameterised models, i.e. MM.

A full account of interactions between the two regions requires introduction of an interface region, the atoms of

* Corresponding author. Fax: +44 20 7670 2920.
E-mail address: sam@ri.ac.uk (S.A. French).

0920-5861/$ – see front matter © 2004 Elsevier B.V. All rights reserved.
doi:10.1016/j.cattod.2004.06.129

which intimately interact both with the QM and MM regions, as discussed in reference [3].

3. Applications

3.1. Methanol synthesis on a model catalyst

In order to study methanol synthesis we first explored areas that provided validation of our model for the active site for catalysis: simulation of polar oxide surfaces of ZnO; their hydrogenation; adsorption of reactants, intermediates and products; characterisation of adsorbed species by their spectroscopic signature; investigation of metal–support interactions and modelling of the formation and oxidation of supported nanoclusters.

The nature of the active site for sorption/catalysis of CO_2 and H_2 on the multicomponent $Cu/ZnO/Al_2O_3$ industrial catalyst still remains unclear. The issues of contention are: (i) What is the source of carbon CO or CO_2? (ii) Which surface is active and which surface sites are involved in the reaction? (iii) What is the role of copper and Al_2O_3? (iv) What is the electronic state of the active site? ([5,6] and references therein).

The clean oxygen terminated surface of zincite was used as a model catalyst. Temperature programmed desorption (TPD) studies have shown that the processes that occur at that particular surface are analogous to those on the real catalyst [7–12]. Therefore, we have first concentrated on issues of catalysis on ZnO.

Vacant oxygen interstitial surface sites (VOISS) were identified as catalytically active sites [4,13]. We have studied the adsorption at VOISS of important methanol precursors including carbon dioxide, formate and methoxy ions and have calculated the equilibrium structure and binding energies of these and related species. The proposed catalytic cycle is summarised in Fig. 1. Interaction with the surface stabilises negatively charged species with both chemisorbed hydrogen and valence ZnO states serving as electron sources. Firstly CO_2 is adsorbed before an electron is transferred resulting in CO_2^-, which is hydrogenated by surface hydrogen to HCO_2^-, the formate anion. Further hydrogenation can proceed either through the formation of $H_2CO_2^-$ or $HCOOH^-$ (formic acid). Production of methoxy and methanol, which is weakly bonded to the surface, is a complex process that includes multiple hydrogenation steps that we have considered separately. To complete the catalytic cycle, methanol is removed from the surface, and the active site is recycled by CO or H_2 scavenging O from the VOISS (leaving $VOISS^-$) and desorbing as CO_2 and H_2O.

The surface binding energies of CO and CO_2 were used in this study for direct comparison with experiment. Experimental desorption energies have been obtained from the low temperature regime of carbon dioxide adsorption as reported by Bowker et al. [8]. During TPD ca. 10% of the adsorbed carbon dioxide dissociates to carbon monoxide and

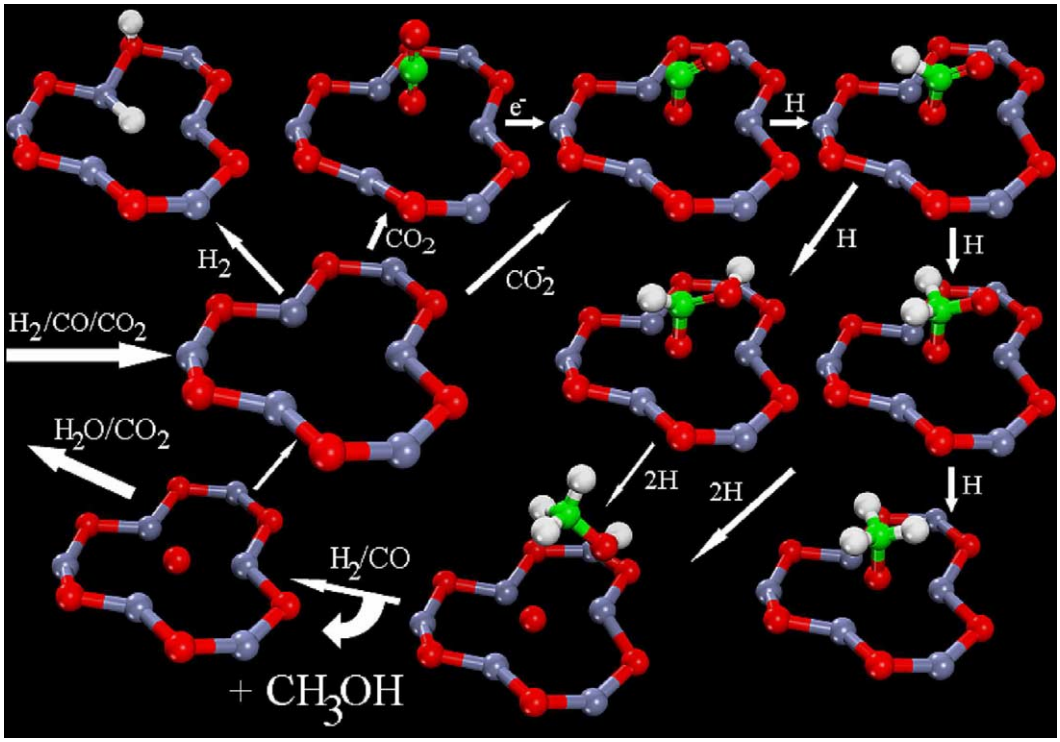

Fig. 1. Catalytic cycle for methanol synthesis from syngas. Pictorial representation of geometry optimised stable reactants, intermediates and products with the portion of surface substrate modelled in the QM region (Grey, zinc; red, oxygen; green, carbon; white, hydrogen).

oxygen that heals the surface defects. Firstly, we calculate 69 kJ mol^{-1} for the abstraction of CO_2 from the VOISS with a trapped electron, which compares to an experimental desorption energy of 109–117 kJ mol^{-1}. Secondly, the energy of desorption of CO is calculated as the energy of cleavage of the O_a–C bond in the CO_2^- adsorbate (as suggested by Bowker) and is found to be 113 kJ mol^{-1}; this value compares favourably with the experimental value of 109 kJ mol^{-1}.

3.2. Supported Group 11 metals on metal oxides

A much improved low temperature methanol synthesis catalyst based on $Cu/ZnO/Al_2O_3$ was introduced in 1965 and now it is well established as the leading industrial catalyst [14]. Despite over three decades of commercial use, many questions remain unresolved concerning the active site of the catalyst. Numerous studies have attempted to tackle these issues employing many different model systems and catalyst preparations.

The synergy between the ZnO support and metal is claimed by many to be the key element in the optimisation of the catalyst. It is therefore of interest to compare different metals and their interaction with ZnO; in this light recent advances in supported gold catalysts are of particular interest. Gold nanoparticles supported on ZnO are active for methanol synthesis [15–17]. IR studies using CO as a probe molecule have confirmed the existence of both metallic and cationic gold nanoparticles on Au/ZnO catalysts [18]. It has been suggested, on the basis of the observed size and support dependency in most gold catalysed reactions, that a very strong metal–support interaction is necessary for high catalytic activity [19]. Silver has also been investigated experimentally for methanol synthesis without conclusive results [20]. Therefore, we have compared all Group 11 metals allowing us to assess the effect of interaction with the support as the property of the metal changes.

Once prepared, catalysts are often pretreated under a number of reducing/oxidising conditions, and finally under reducing conditions at high temperatures (200–300 °C). These pretreatments can leave M^+ and M^{2+} ions at the surface of the catalyst both stabilised in metal oxides and/or atomically dispersed on the ZnO surface [21–24]. We have used the vacant zinc interstitial surface sites (VZISS) at the Zn terminated polar surface of ZnO as it presents an ideal environment for anchoring metals. Stabilisation of the charged species in the anchor site is achieved when its HOMO level lies below the bottom of the surface conduction band (CB) while its LUMO level is above the top of the valence band (VB).

The surface electrostatic potential at the VZISS results in an upward shift of all electronic levels of the adsorbed species. The magnitude of the shift strongly depends on the position of the metal ion over the surface as the potential decays exponentially with the height. Thus, the anchor atom of a metal cluster experiences a distinctly different electrostatic potential from that experienced by other metal atoms adsorbed on top of it. This difference in the electrostatic potential provides a rationale for the observed partially cationic state of supported metal clusters.

Table 1
The calculated HOMO and LUMO values for single anchor atoms

Species	HOMO (eV)	LUMO (eV)	Height (Å)
Cu^0	−2.028	−0.812	0.871
Cu^{1+}	−5.578	−1.789	0.319
Cu^{2+}	−10.141	−6.434	0.014
Ag^0	−2.119	−0.534	1.48
Ag^{1+}	−5.920	−1.223	0.881
Ag^{2+}	−11.329	−8.923	0.36
Au^0	−3.400	−1.837	1.587
Au^{1+}	−6.814	−2.265	0.496
Au^{2+}	−9.696	−6.964	0.320
ZnO surface	−5.49	−2.12	0

The LUMO level of ZnO surf is shifted from the top of the VB by the experimental band gap value, 3.4 eV.

Here, we concentrate on the stability and electronic state of the anchor. Three elements considered, Cu, Ag and Au, all have a $d^{10}s^1$ electronic ground state in vacuo. In neutral and singly ionised states the respective atoms are stabilised on an approximate symmetry axis of the VZISS, along the surface normal, at heights in accordance with their radii. The first ionisation potential for stripping an outer s electron behaves non-monotonically in this series (7.7, 7.6 and 9.2 eV, respectively) [25].

From Table 1 it can be seen that our calculations predict that the most likely anchor species are M^+ species as all those studied are stable at the VZISS site. The HOMO level of Au^0 is also lower than the CB of the surface, and therefore, the species is stable. Cu^0 and Ag^0 are seen to be electron donors as their HOMO levels are calculated to be above the estimated position of the bottom of the CB, with the potential for spontaneous or thermally assisted ionisation (Fig. 2).

As can be expected, on further ionisation, the ions sink deeper into the surface, which further destabilises their electronic states. The resulting shift is however insufficient, leaving their LUMO below the top of the surface valence band, which leads to electron transfer from the valence band to the metal. Interestingly, the transfer occurs not into an open d shell of these ions, but to an s level. Upon adsorption the d^9 ion forms a (d^9s^1, h^+) electronic state with the hole delocalised over the second and further neighbours. Detailed analysis for copper is given in [26].

We have also examined the stability of Cu^+, Cu^{2+}, Ag^+, Ag^{2+}, Au^+ and Au^{2+} as substitutionals for Zn^{2+} on the bulk-terminated island site of the ZnO(0 0 0 1) surface. The higher oxidation states were found to be stable as they all lie within the HOMO–LUMO gap of ZnO, which points at the potential stability of such species in agreement with experiment. This result is an indication that gold cations can exist as impurities on the surface of ZnO. We are currently investigating the nucleation energetics and structures of supported Au_n clusters, in addition to our previously published

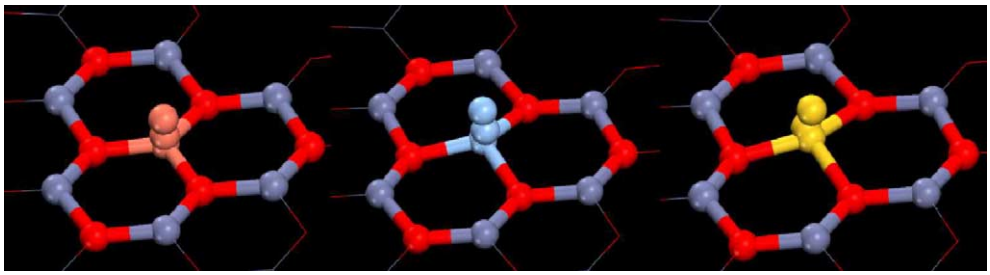

Fig. 2. Left: Cu, centre: silver, right: gold. For all metals it can be seen that M^0 sits higher than M^{1+}, while M^{2+} sits in the surface plane.

Table 2
HOMO and LUMO values for metal ions substituted into the island site on the ZnO surface

Species	HOMO(eV)	LUMO(eV)	Height (Å)
Cu^{1+}	−2.176	1.750	0.333
Ag^{1+}	−3.557	1.695	0.743
Au^{1+}	−3.165	0.614	0.678
Cu^{2+}	−2.176	1.750	0.138
Ag^{2+}	−5.353	−3.248	0.272
Au^{2+}	−5.382	−2.795	0.304
ZnO surface	−5.473	−2.103	0

The LUMO level of ZnO surf is shifted from the top of the VB by the experimental band gap value, 3.4 eV.

work on Cu_n clusters [26], to understand how the metal oxide may influence metal atoms (Table 2).

We conclude that straight metal deposition on the (0 0 0 1)-Zn surface of ZnO is unlikely to result in stabilisation of the metal in oxidation state II. An intriguing insight is however given by considering particular preparations of the catalyst by metal deposition from aqueous solutions. The higher oxidation states are, for example, accessible when Au adsorbs as an $Au(OH)_x$ species at the VZISS.

3.3. Functional metal centres in the zeolite framework

Crystalline structures of the zeolite type, but with elements other than or in addition to silicon and aluminium can be introduced into the framework by direct hydrothermal synthesis or by post synthesis isomorphous substitution [27]. One of the most successful examples of an isomorphous substituted zeolite is the highly efficient and selective catalyst Ti-silicalite, TS-1. TS-1 is well known for its outstanding ability to catalyse various industrially important oxidation reactions such as the hydroxylation of phenol, epoxidation of olefins and the ammoximation of cyclohexanone, under mild conditions with aqueous H_2O_2 as the oxidant [28]. The catalytic activity of TS-1 has been attributed to the presence of isolated tetrahedrally coordinated Ti sites in silicalite and to certain characteristics of the zeolite itself such as the channel dimensions and hydrophobic character.

The success of TS-1 in industrial catalytic processes has stimulated the search for catalysts containing elements other than Ti in the silica lattice with the same coordination and environment. In particular, the isomorphous replacement of Si by tetravalent elements that are positioned in the same column as silicon (Group 14) and titanium (Group 4) in the periodic table, have attracted much attention since they are expected to exhibit similar catalytic properties. For instance considering the elements in Group 14, Sn containing silicalite (Sn-Sil-1) prepared by hydrothermal synthesis with $SnCl_4$ [29] has been used as a catalyst in the hydroxylation of phenol with aqueous H_2O_2 [30]. It appears that the selectivity of products is different between Sn-Sil-1 and TS-1 depending on the nature of the solvent used during the reaction. Similar to Sn-Sil-1, Zr substituted silicalite has been synthesised hydrothermally, with $ZrCl_4$ aqueous solution as the zirconium source [31]. Although, not yet applied as an industrial catalyst, there is evidence that Ge can be incorporated into silicalite, and, for example, recently a new pure silica zeolite ITQ-7 has been synthesised with substitution of framework Si by Ge [32,33].

In general, there are two requirements, which have to be fulfilled in order to incorporate elements into the zeolite framework. The first requires that the substituted element must be approximately the size of the atoms it replaces (i.e. Si), and the second states that the substituted element must be able to coordinate in a tetrahedral position in the framework.

Neutron diffraction studies have investigated the distribution of Ti atoms in the MFI framework [34,35] and reported that the occupancy of Ti at the framework T8 site was preferred in the orthorhombic unit cell of silicalite. For this reason we selected the T8 site as a promising candidate for isomorphous substitution.

A QM/MM cluster of 18 Å radius with the T8 atom located at the centre was used to represent the zeolite system. Atoms within three coordination spheres of T8 are treated quantum mechanically, and a total of 38 atoms, including all the QM atoms are optimised. Optimisation calculations were performed at the B3LYP level with TZVP basis sets at the T site and DZP basis sets on all other QM centres, followed by single point calculations with an extended TZV_2P basis set on the T8 atom [36]. Effective core potentials were used for the heavier elements such as Sn, Pb, Zr and Hf [37].

We have compared bond lengths and substitution energies with ionic radii [25] and found clear correlation. Fig. 3 shows that the calculated average T–O bond length increases with the increasing size of the T8 atom.

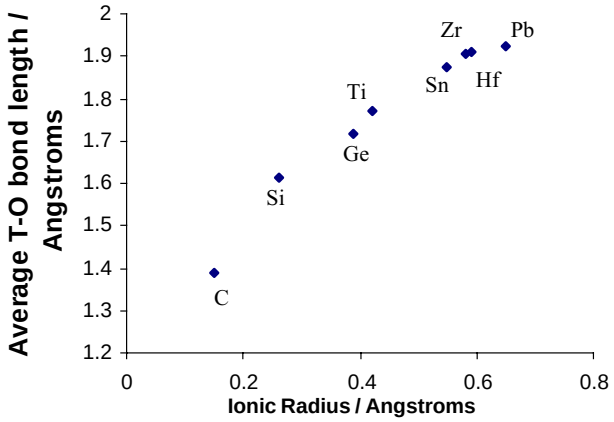

Fig. 3. Average T–O bond lengths with respect to the ionic radius of T8 atom.

The stability of each of the elements substituted into the T8 site of the silicalite was estimated relative to the pure siliceous system, following the reaction:

$$SiO_2 + MCl_4(g) \leftrightarrow MO_2 + SiCl_4(g)$$

The calculated substitution energies for the optimised clusters are displayed in Fig. 4, and for comparison the elements of the same row of the periodic table are paired next to each other.

Fig. 4 shows that more energy is required to substitute a Group 14 element for Si than a Group 4 element in the same row. Further analysis shows that the substitution energy does not increase uniformly for Group 4 elements as we move down the group, for example, Hf has a similar substitution energy to the lighter Zr. This is attributed to the lanthanide and relativistic contractions, which occur in the heavier element, Hf, which is further supported by the fact that Zr (fourth row) and Hf (fifth row) have similar ionic radii. The effect is much less pronounced for Pb since it has a full outer d shell, which is subject to less contraction.

From our calculations it is clear that the ionic radius governs the ability of an ion to enter the zeolitic framework,

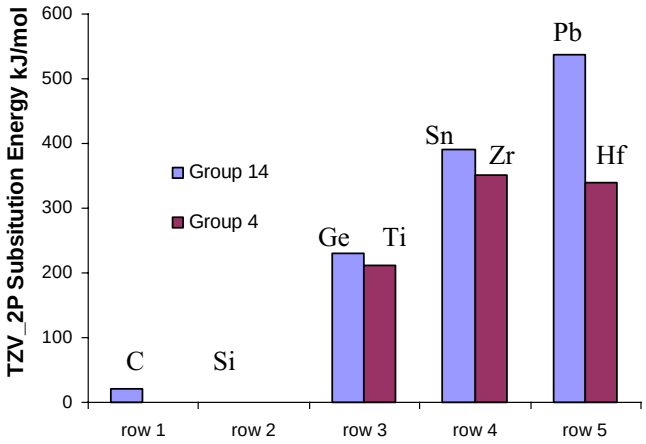

Fig. 4. Substitution energies for Groups 4 and 14 QM/MM clusters.

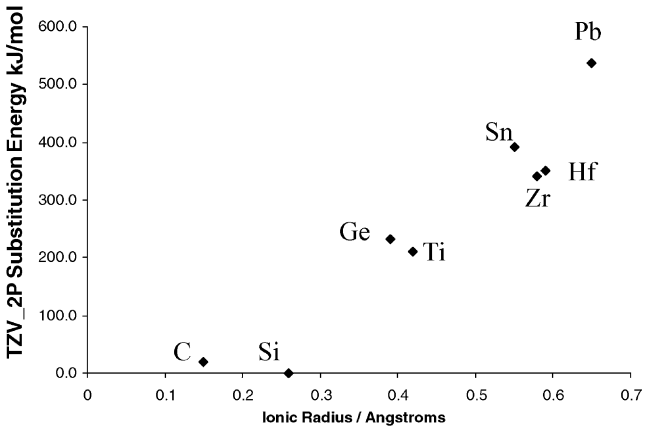

Fig. 5. Substitution energy with respect to ionic radius of T8 atom.

as shown in Fig. 5. Clear trends are shown when comparing both substitution energies and bond lengths. As Zr-Sil-1 has been synthesised our calculations would predict that it should be possible to prepare analogous Hf zeolites.

4. Conclusions

Our methodology clearly has the ability to elucidate a detailed and quantitative mechanism for the catalytic processes involved in the synthesis of methanol and provide insights into electronic structure, properties and stability of dopants on internal and external surfaces of solid supports for heterogeneous catalysis.

Acknowledgements

We thank ICI/Synetix, EPSRC, Accelrys and Royal Society for support and funds. For many useful discussions and support we are indebted to our colleagues, particularly P. Sherwood and A. Beale. For more information on availability of the software employed in these studies please see the web site http://www.cse.clrc.ac.uk/qcg/quasi.

References

[1] P. Sherwood, A.H. de Vries, S.J. Collins, S.P. Greatbanks, N.A. Burton, M.A. Vincent, I.H. Hillier, Faraday Discuss. 106 (1997) 79.
[2] A.A. Sokol, S.T. Bromley, S.A. French, C.R.A. Catlow, P. Sherwood, A hybrid QM/MM embedding approach for the treatment of localised surface states in ionic materials, Int. J. Quantum Chem. (2004), in press.
[3] P. Sherwood, A.H. de Vries, M.F. Guest, G. Schreckenbach, C.R.A. Catlow, S.A. French, A.A. Sokol, S.T. Bromley, W. Thiel, A.J. Turner, S. Billeter, F. Terstegen, S. Thiel, J. Kendrick, S.C. Rogers, J. Casci, M. Watson, F. King, E. Karlsen, M. Sjøvoll, A. Fahmi, A. Schäfer, Ch. Lennartz, J. Mol. Struct. (Theochem.) 632 (2003) 1.
[4] S.A. French, S.T. Bromley, A.A. Sokol, C.R.A. Catlow, S.C. Rogers, F. King, P. Sherwood, Angew. Chem. 113 (2001) 4569.
[5] E.I. Solomon, P.M. Jones, J.A. May, Chem. Rev. 93 (1993) 2623.

[6] G.C. Chinchen, P.J. Denny, D.G. Parker, M.S. Spencer, D.A. Whan, Appl. Catal. 30 (1987) 333.
[7] V.E. Heinrich, P.A. Cox, The Surface Science of Metal Oxides, Cambridge University Press, Cambridge, 1996.
[8] M. Bowker, H. Houghton, K.C. Waugh, J. Chem. Soc. Faraday Trans. 1 (77) (1981) 3023.
[9] K.M. Vandenbusche, G.F. Froment, Appl. Catal. A 112 (1994) 37.
[10] S. Bailey, G.F. Froment, J.W. Snoeck, K.C. Waugh, Catal. Lett. 30 (1995) 99.
[11] I. Nakamura, H. Nakano, T. Fujitani, T. Uchijima, J. Nakamura, Surf. Sci. 404 (1998) 92.
[12] K.R. Harikumar, C.N.R. Rao, Appl. Surf. Sci. 125 (1998) 245.
[13] S.A. French, A.A. Sokol, S.T. Bromley, C.R.A. Catlow, S.C. Rogers, P. Sherwood, J. Chem. Phys. 118 (1) (2003) 317.
[14] J.M. Thomas, W.J. Thomas, Principles and Practice of Heterogeneous Catalysis, Wiley-VCH, Weinheim, 1996.
[15] H. Sakurai, S. Tsubota, M. Haruta, Appl. Catal. A: Gen. 102 (1993) 125.
[16] H. Sakurai, M. Haruta, Appl. Catal. A: Gen. 127 (1995) 93.
[17] H. Sakurai, M. Haruta, Catal. Today 29 (1996) 361.
[18] F. Boccuzzi, A. Chiorino, S. Tsubota, M. Haruta, Sens. Actuators B 24–25 (1995) 540.
[19] G.C. Bond, D.T. Thompson, Catalysis by Gold, Catal. Rev.—Sci. Eng. 41 (3/4) (1999) 319.
[20] S. Sugawa, K. Sayama, K. Okabe, H. Arakawa, Energy Convers. Manage. 36 (1995) 665.
[21] G. Meitzner, E. Inglesia, Catal. Today 53 (1999) 433.
[22] J. Nakamura, T. Uchijima, Y. Kanai, T. Fujitani, Catal. Today 28 (1996) 223.
[23] H.Y. Chen, S.P. Lau, L. Chen, J. Lin, C.H.A. Huan, K.L. Tan, J.S. Pan, Appl. Surf. Sci. 152 (1999) 193.
[24] Y. Izumi, F. Kiyotaki, H. Nagamori, T. Minato, J. Electron. Spectrosc. Relat. Phenom. 119 (2001) 193.
[25] D.R. Lide (Ed.), CRC Handbook of Chemistry and Physics, CRC Press, London, 2003.
[26] S.T. Bromley, S.A. French, A.A. Sokol, C.R.A. Catlow, P. Sherwood, J. Phys. Chem. B 107 (29) (2003) 7045.
[27] A. Corma, J. Catal. 216 (2003) 298.
[28] R.K. Grasselli, A.W. Sleight, Structure–Activity and Selectivity Relationships in Heterogeneous Catalysis, Elsevier Science, Amsterdam, 1991, p. 243.
[29] P. Fejes, J.B. Nagy, K. Kovacs, G. Vanko, Appl. Catal. A 145 (1996) 155.
[30] N.K. Mal, A.V. Ramaswamy, J. Mol. Catal. A 105 (1996) 149.
[31] B. Rakshe, V. Ramaswamy, S.G. Hegde, R. Vetrivel, A.V. Ramaswamy, Catal. Lett. 45 (1997) 41.
[32] A. Corma, M.J. Diaz-Cabanas, H. Garcia, E. Palomares, Chem. Commun. (2001) 2148.
[33] T. Blanco, A. Corma, A.J. Diaz-Cabanas, F. Rey, J.A. Vidal-Moya, C.M. Zicovich-Wilson, J. Phys. Chem. B 106 (2002) 2634.
[34] S. Bordiga, S. Coluccia, C. Lamberti, L. Marchese, A. Zecchina, J. Phys. Chem. 98 (1994) 4125.
[35] C.A. Hijar, R.M. Jacubinas, J. Eckert, N.J. Henson, P.J. Hay, K.C. Ott, J. Phys. Chem. B 104 (2000) 12157.
[36] A. Schäfer, H. Horn, R. Ahlrichs, J. Chem. Phys. 97 (1992) 2571; A. Schäfer, C. Huber, R. Ahlrichs, J. Chem. Phys. 100 (1994) 5829.
[37] M. Dolg, U. Wedig, H. Stoll, H. Preuss, J. Chem. Phys. 86 (1987) 866.